



A narrowband virtual sensing Active Noise Control system using ESPRIT for an aircraft interior.

Erspamer A., Mylonas D., Yiakopoulos C., Antoniadis I.

National Technical University of Athens, School of Mechanical Engineering, Department of Mechanical Design & Automatic Control, Laboratory of Dynamics and Structures, Athens, Greece.

Abstract

In present work, an Active Noise Control system is proposed, aimed at the attenuation of low frequency, periodic noise. This type of noise, that is produced by internal combustion engines of vehicles is a serious problem due to low efficiency of traditional, passive sound insulation methods. Besides that, it can produce fatigue and lack of concentration to humans who are exposed for long periods. The 3 input/4 output multichannel ANC system presented in this work, consists of three parallel notch filters. Each of them is responsible for the attenuation of one tone of the noise of interest. Moreover, ESPRIT algorithm is used to estimate the frequencies of these periodic noise components. Finally, a forward difference prediction technique is proposed for the relocation of the quiet zone from the space around the physical microphones to an area far from them. This result is important for a headrest system of a vehicle's seat because it is usually inconvenient to place physical sensors around passengers' ears. The developed ANC structure has been tested by extensive experiments of a synthetic low frequency tonal and beat noise in a small wooden aircraft's cabin mockup. The experimental results show that an important reduction of the overall SPL is achieved around the virtual locations determined by sound pressure extrapolation technique. The quiet zone being formed is large enough to ensure freedom of movement of passenger's head. In addition, the frequency estimation through ESPRIT technique is fast enough to ensure the convergence of control algorithm and to minimize frequency mismatches.

Keywords: active noise control; adaptive notch filter; virtual sensing; first-order pressure prediction technique; ESPRIT.

1 Introduction

Low frequency harmonic noise is a serious problem for small single engine aircraft cabins because not only can cause damage to passengers' and pilots' hearing but also leads to fatigue, feeling of discomfort and loss of concentration for long periods of exposure. This noise is mainly consisted of the first three harmonics of the propeller's Blade Passage Frequency (BPF) and is transmitted to the cabin through several paths, including the engine mounts into the wing structure and the fuselage [1]. While noise of higher frequencies may be reduced using passive techniques, the longer wavelength associated with low frequencies would lead to impractically large and massive sound insulating structures. Moreover, this kind of structures do not comply with the actual trend of making lighter aircrafts that consume less fuel and as a result are more environmentally friendly [2]. To overcome the issues above Active Noise Control (ANC) techniques have attracted considerable interest. Several attempts have been made in the direction of making a robust ANC system that creates an adequate quiet zone around the ears of an aircraft's passenger and some of them have been developed into commercial applications [3]. Most of them are based on Filtered-x Least Mean Square algorithm which is widely used for noise level reduction applications due to its robustness and low computational complexity. Siswanto et al. [4] proposed a two-input two output ANC headrest system using multichannel feedback FxLMS

algorithm with satisfactory results regarding the quiet zone created around the passengers' ears. Moreover in [1,5] different approaches of multichannel ANC systems are presented for the cabins of light aircrafts. The differences are associated with the kind of the control method (feedforward or feedback) and the number of sensors and actuators used for the system's implementation. In addition, much research has been made on adaptive notch filters connected in parallel for low frequency noise attenuation. Wang et al. [6] adopted a multi-tone ANC system to control a signal constituted by three tones and broadband noise. Similar attempts with considerable results have been made in [7,9]. However, none of these studies present results regarding the size of the quiet zone which is created. In the present research a multi-tone narrowband ANC system based on parallel adaptive notch filters [8] is proposed in order to enhance the noise attenuation levels inside an extended quiet zone, around the ears of an aircraft's passenger. The main approach to do so is the integration of an extrapolation-based virtual sensing technique in the traditional multichannel FxLMS algorithm to update the weights of the notch filters. Each notch filter is responsible for the attenuation of a single tone. Moreover, the extrapolation-based virtual sensing technique, based on the first-order pressure prediction, can expand this attenuation forming a large quiet zone. Additional issues that arise in multi-tone ANC systems based on adaptive notch filters are related with the method used for the estimation of the reference signal's frequencies and the performance degradation caused by the frequency mismatches. A simple frequency estimator that counts the time between zero crossings is presented in [8]. In [6] a parallel adaptive notch filter algorithm is proposed to obtain accurate frequency estimation which is used to create reference signals. A narrowband ANC system structure with an FIR filter as a magnitude phase adjuster is also made to cope with frequency mismatches in [10]. Finally, another narrowband ANC scheme that incorporates a frequency estimator which deals with reference frequency mismatches is proposed by Jeon et al. in [9]. In current work a frequency estimator that uses parametric frequency estimation method ESPRIT is proposed to track the frequency changes of the reference signals. The developed multi-tone ANC structure, using ESPRIT has been tested with real-time experiments in an aircraft cabin mockup under synthetic, low frequency tonal and beat noise which simulates the noise produced by the engines of a small aircraft. The experimental results demonstrate that proposed system creates a large quiet zone around passengers' ears with significant attenuation of BPF. The size of the quiet zone and the attenuation of narrowband noise are presented in detailed diagrams. Moreover, the results show that frequency estimation is fast and accurate enough to ensure the stability and convergence of the proposed ANC algorithm.

2 Algorithm analysis

2.1 Multichannel Narrowband ANC

The ANC system presented in this work is based on three parallel multichannel sub-systems. Each of them is responsible for the attenuation of one sinusoidal component of the noise produced by the aircraft's propeller, acting as an adaptive notch filter. As a result, the proposed system can control up to 3 harmonics. In addition, it can be expanded depending on the available hardware resources. J reference signals are obtained by creating a cosine waveform for each frequency

$$x_j(n) = A_j \cos(\omega_j n), \quad j = 1,2,3 \quad (1)$$

The adaptation algorithm is single reference/ multiple-input/ multiple-output FxLMS. More specifically three error signals are used for the adaptation process and four output signals are produced, one for each loudspeaker (Fig. 1). The iterative equation of MIMO FxLMS algorithm that updates the filter weights can be expressed as

$$w_{kj}(n+1) = w_{kj}(n) + \mu \sum_{m=1}^3 x'_{jkm}(n) e_m, \quad k = 1, \dots, 4. \quad (2)$$

where

$$x'_{jkm} = \hat{s}_{mk} * x_j(n) \quad (3)$$

Each reference input is filtered by the secondary path estimate \hat{s}_{mk} that is the electroacoustic path between m ($m=1,2,3$) error microphone and k ($k=1, \dots, 4$) loudspeaker. Finally, the driving signal for each loudspeaker is the sum of 3 adaptive filters' outputs, if the sound disturbance consists of three main frequencies (Fig. 1):

$$y_k(n) = \sum_{j=1}^3 y_{kj}(n) \quad (4)$$

and

$$y_{kj}(n) = \sum_{l=0}^{L-1} w_{kj}(n) x_j(n-l), \quad L = 10. \quad (5)$$

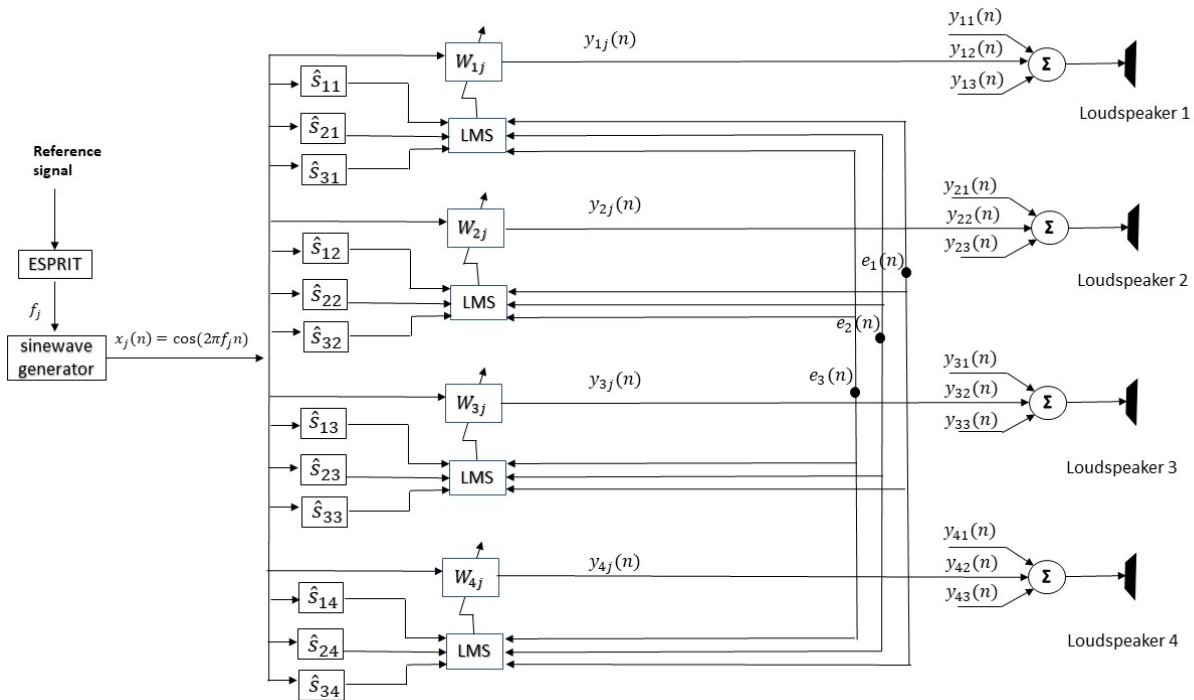


Figure 1- Single reference/ Multiple Input/ Multiple Output ANC subsystem for the attenuation of a single sinusoid. Three such subsystems are included in the total system.

2.2 Relocation of quiet zone

The ANC scheme presented above can create an efficient quiet zone around the physical error microphones. However, in a real system it is inconvenient to mount the sensors around the passenger's ears. As a result, a relocation of the quiet zone is necessary. In a 3D enclosure, under a low frequency noise (<500 HZ) the change of pressure for closely spaced locations in terms of wavelength is small. Thus, in this case the sound pressure at a virtual location (ear) can be estimated in real time by fitting a polynomial to the measured sound pressures from an array of physical error microphones (Fig. 2a), which are installed sequentially one after the other in the same direction and horizontal plane, and then extrapolating the produced line or curve to a virtual location [11]. In this work, a first order polynomial has been used to estimate the sound pressure at distances x between the virtual and the nearest physical error microphone (Fig. 2b). The sound pressure at the virtual position has been calculated from equation (6).

$$\hat{e}_v(n) = \frac{e_{p2}(n) - e_{p1}(n)}{a}x + e_{p2}(n) \quad (6)$$

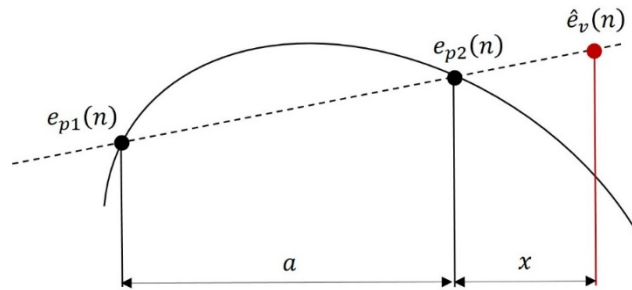


Figure 2- Estimation of the acoustic pressure at virtual location through a linear extrapolation technique.

Then the sum of the estimated pressures has been put in equation (2) to create a relocated quiet zone around the estimated sensors. We can also assume that the secondary paths of the virtual sensors are approached by \hat{s}_{pk} . This result can be obtained, if we consider that the acoustic path between the physical and the virtual sensors is a pure delay with impulse response

$$h(n) = \delta(n - D) \quad (7)$$

Thus, the secondary path for the virtual sensor would be

$$\hat{s}_{mk}^{virtual} = \hat{s}_{mk} * \delta(n - D) \quad (8)$$

and the reference signals filtered by the “virtual” secondary paths would be

$$x'_{jkm} = \hat{s}_{mk} * x_j * \delta(n - D) = \hat{s}_{mk} * x_j(n - D) \cong \hat{s}_{mk} * x_j(n) \quad (9)$$

The assumption above can be made for sinusoids with big wavelengths and for a small distance between physical and virtual sensors. In this case the delay D is less than one sample, and the values of acoustic pressure are almost same.

2.3 ESPRIT algorithm

ESPRIT algorithm, which was proposed by Paulraj et al. [12] is a very efficient algorithm with relatively low computational complexity that is used to estimate important parameters of a signal like the number of sources and DOA's. For the ANC system being presented in the current research, ESPRIT has been used to estimate

the frequencies produced by aircraft's propeller that are embedded in a noisy signal. Below the steps of the algorithm are briefly presented:

1. Compute the covariance matrices R_{yy} and R_{yz} , where $y(n)$ is the reference signal being obtained by a physical sensor and $z(n)=y(n+1)$.
2. Define the eigenvalues of R_{yy} . For $M > p$, where M is the length of the input buffer and p is the number of embedded sinusoids, the minimum eigenvalue is an estimation of σ_w^2 , where $w(n)$ is the noise component of $y(n)$.

3. Compute matrices $\hat{C}_{yy} = R_{yy} - \hat{\sigma}_w^2 I$ and $\hat{C}_{yz} = R_{yz} - \hat{\sigma}_w^2 Q$, where $Q = \begin{bmatrix} 0 & 0 & 0 & \dots & 0 & 0 \\ 1 & 0 & 0 & \dots & 0 & 0 \\ 0 & 1 & 0 & \dots & 0 & 0 \\ \cdot & \cdot & \cdot & \ddots & \cdot & \cdot \\ \cdot & \cdot & \cdot & \cdot & \cdot & \cdot \\ \cdot & \cdot & \cdot & \cdot & \cdot & \cdot \\ 0 & 0 & 0 & \dots & 1 & 0 \end{bmatrix}$.

4. Define the generalized eigenvalues of the matrix pair $\{\hat{C}_{yy}, \hat{C}_{yz}\}$. There are p eigenvalues on the unit circle (or near it), which are the estimation of the reference signal frequencies. [14]

3 Experimental analysis

3.1 Experimental setup

As mentioned in paragraph 2.1, the proposed ANC system consists of 4 medium-sized control loudspeakers model Visaton FR 6,5 and 3 pairs of microphones model MX183 Shure (Fig. 3a).

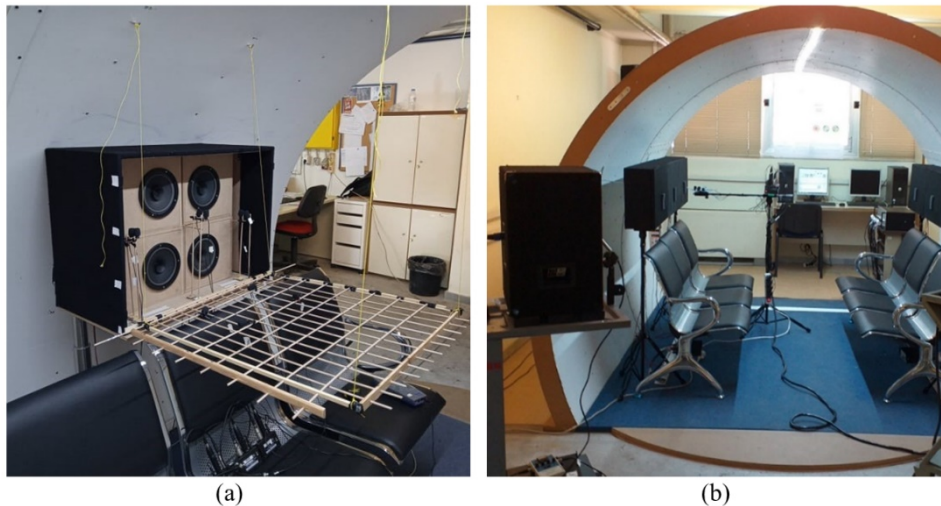


Figure 3- (a) the hardware configuration of the ANC system and the grille used to measure the size of the quiet zone (b) and the wooden cabin mockup.

The control algorithm was implemented in a NI cRIO-9030 controller using LabView FPGA platform. The cRIO utilizes an embedded Xilinx Kintex-7 FPGA with a 40 MHz clock. The sampling of the error microphones has been made through a NI 9220 analog input module and the digital to analog conversion through a NI 9264 analog output module. The whole system has been installed inside a cabin mockup made of wood, 2m high and with radius equal to 1.375m (Fig. 3b). The details and the dimensions of the ANC system configuration are shown in figure 4.

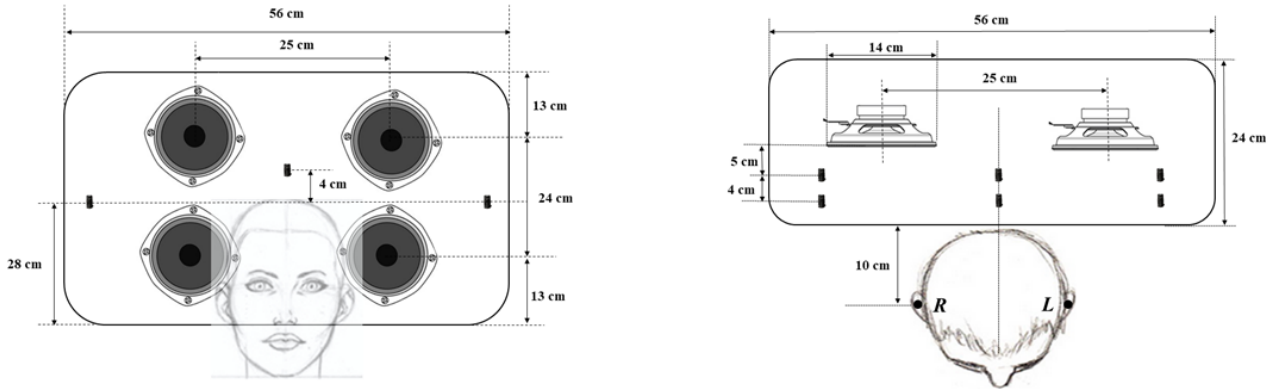


Figure 4-Front view and top view of the proposed ANC system configuration.

In addition, the synthetic sound disturbance, that simulates the noise produced by the propellers of a small aircraft has been created in LabView platform and reproduced by a subwoofer model Omnitronix BX 1250 driven by a power amplifier model Behringer KM750. Finally, a reference microphone model MX183 Shure has been placed in front of the subwoofer and 10 cm far from it to “feed” ESPRIT technique and to obtain the tones embedded in the noise.

3.2 Performance of ANC system

The ANC system was tested for a signal with one harmonic at 110 Hz and a beat signal with two frequencies at 110 Hz and 114 Hz. To simulate better the sound disturbance produced by a small aircraft, a 30db Gaussian noise was added to the final signal. The SPL distribution on a horizontal and flat test area $A = 0.4 \times 0.5 \text{ m}^2$ is calculated mounting observation microphones on a wooden grille (Fig. 3a). A vertical displacement of this grille was applied to build a 3D measurement grid consisting of four flat planes. The separating distance between two planes was 10 cm. First plane’s position was set to be at level 10 cm from the base of the lower loudspeakers. For clarity reasons we should say that in the figures that follow there are no SPL measurements for a small distance in front of the loudspeakers because this area is not accessible by the passenger’s ears.

The parameters of the adaptation algorithm (Eq. 2) have been tuned to ensure fast convergence and stability. The step size has been chosen equal to $\mu = 1e - 5$ and the notch filter taps equal to $N=30$. In addition, the parameter x for the linear extrapolation technique was set to 12 cm.

In the case of one tone signal while ANC system is off, the overall SPL varied from 80db to 85db at the four different planes. Then the system was activated and the reduction of the SPL is shown in figure 5. Especially for planes B and C (20cm and 30cm from the base of lower loudspeakers) a significant sound attenuation of 18db to 25db is achieved up to 20cm far from the loudspeakers. Moreover, an SPL reduction of 6db to 12db has been achieved for 30cm far from the headrest for the planes mentioned above. The system’s performance at these levels is important because it coincides with the ear level of a passenger around 175cm to 185cm. The noise attenuation gets worse at planes A and D (3db to 9db). Thus, the quiet zone is spread over a space of

volume $V = 0.4 \times 0.3 \times 0.3 \text{ m}^3$ ($W \times L \times H$) which is adequate for the movements of a passenger around the headrest.

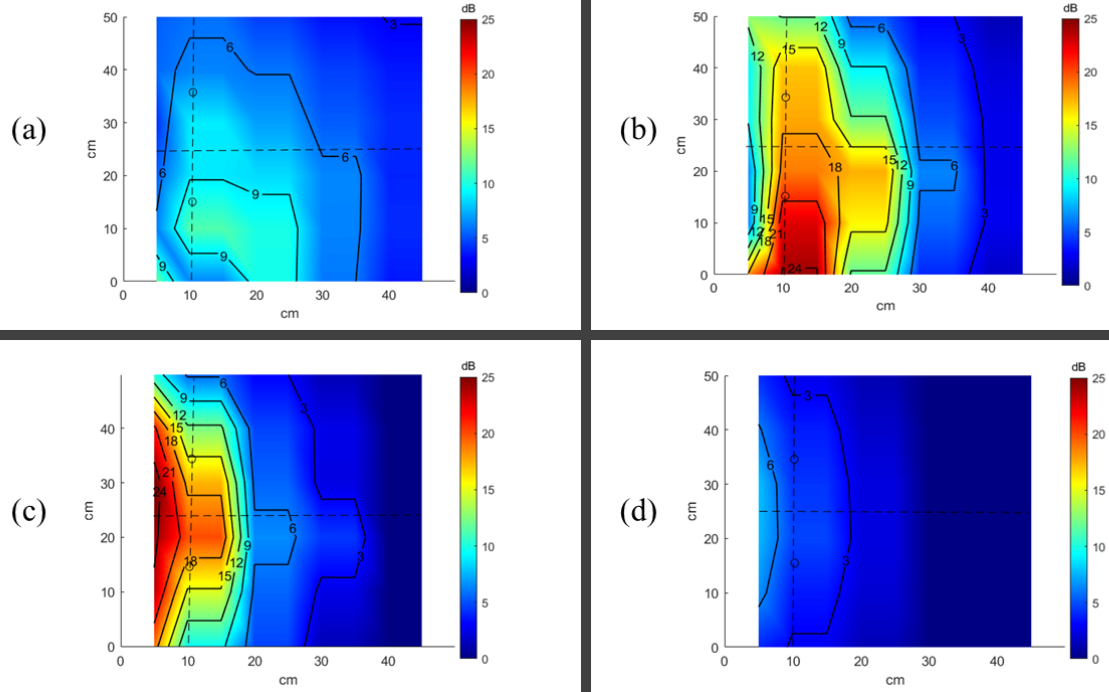


Figure 5- Total SPL difference before and after the ANC activation at different horizontal contours (a) A plane, (b) B plane, (c) C plane, (d) and D plane. The ‘o’ indicates the basic location of the ears.

The significant attenuation of the harmonic at 110 Hz is also depicted in the spectrums of figure 6.

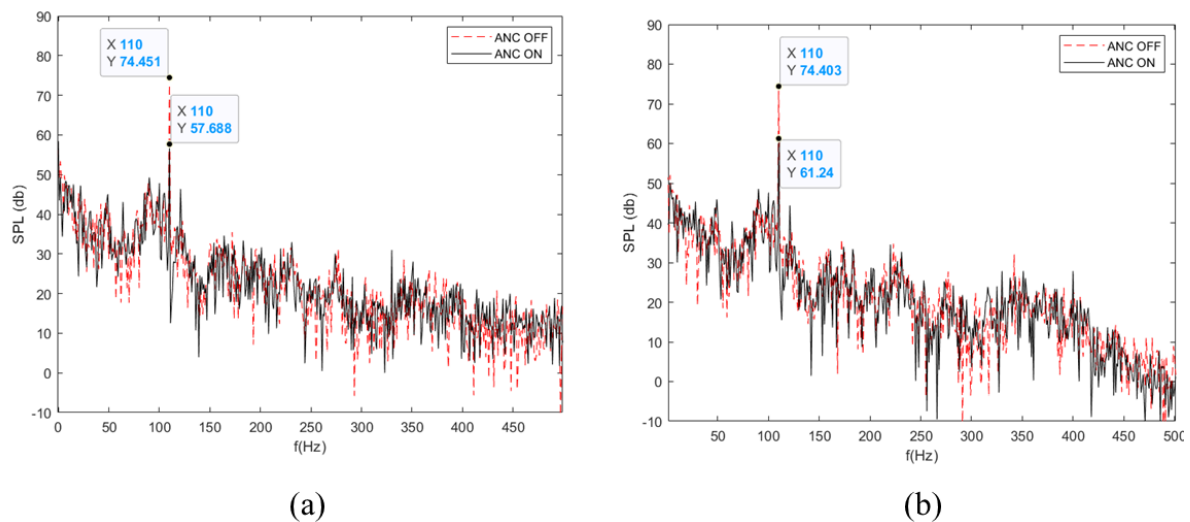


Figure 6- Spectrums of monitoring signals close to the (a) left and (b) right ear of an 175 cm person (B plane) while the ANC system using the proposed methodology is off (red dot line) and on (black line).

In the second experiment the proposed ANC system was analyzed for a beat signal with two frequencies at 110 Hz and 114 Hz, that simulates the sound produced by two non-synchronized engines of a propeller aircraft. The algorithm parameters remained the same as in the first experiment. The only difference is that in the case

of the beat signal has been used two parallel adaptive notch filters, each for the attenuation of one frequency. The overall SPL at four planes before the activation of ANC varied from 79 db to 82 db and the overall SPL reduction achieved by the ANC is depicted in figure 7.

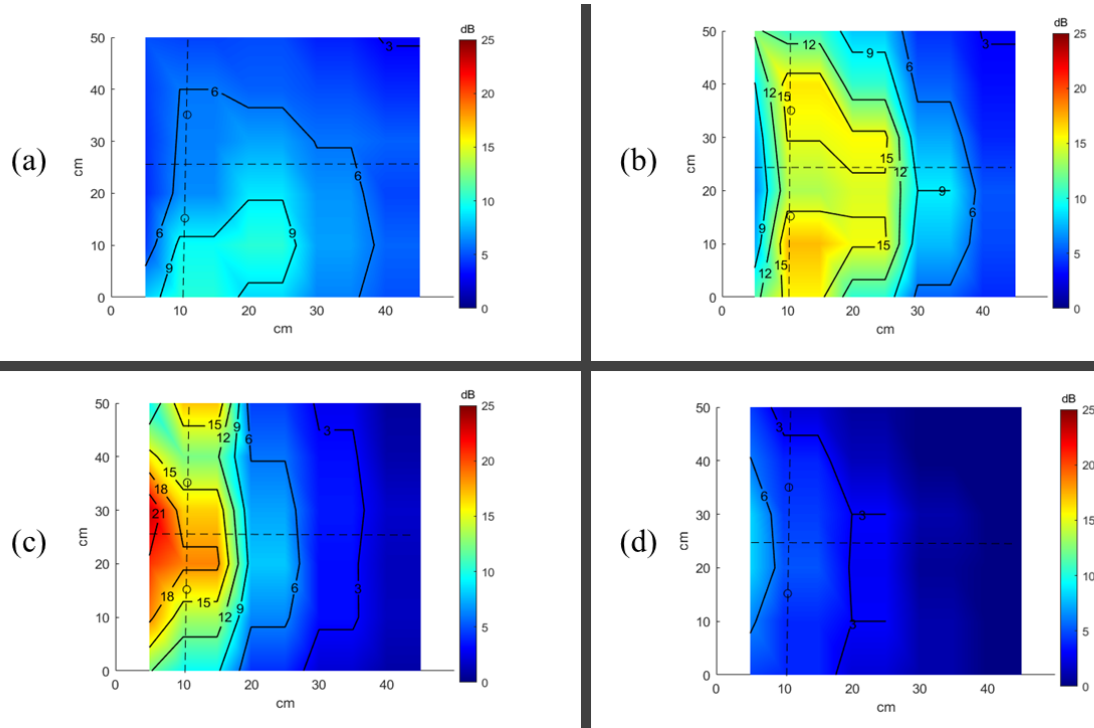


Figure 7- Total SPL difference before and after the ANC activation at different horizontal contours in the case of beat signal (a) A plane, (b) B plane, (c) C plane, (d) and D plane. The ‘o’ indicates the basic location of the ears.

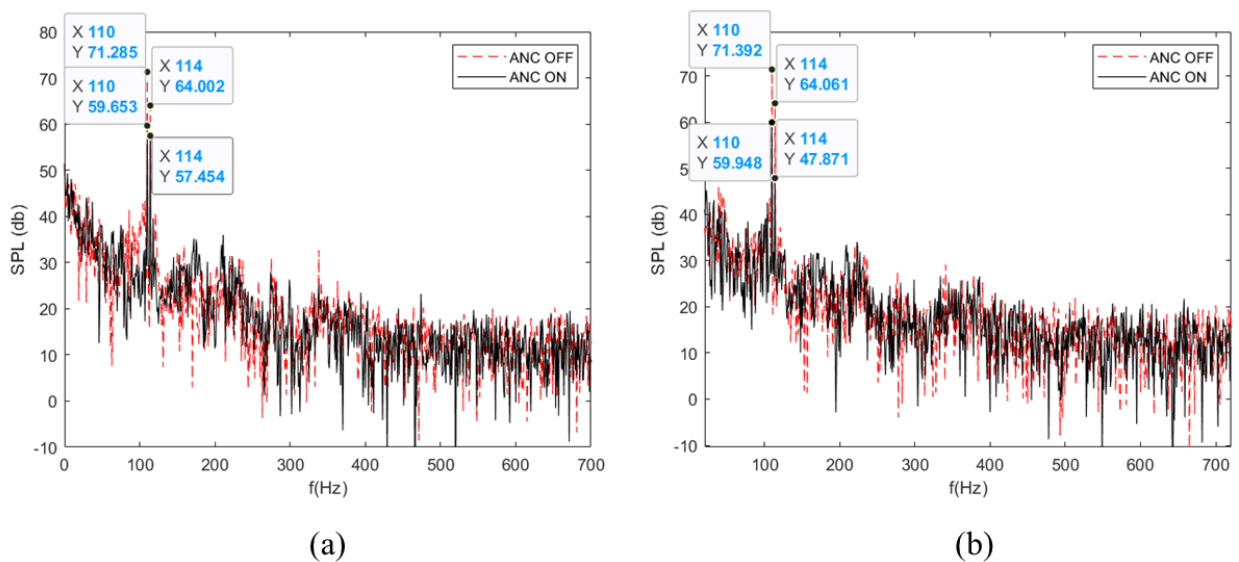


Figure 8- Spectrums of monitoring signals close to the (a) left and (b) right ear of a 175 cm person (B plane) while the ANC system using the proposed methodology is off (red dot line) and on (black line).

In figure 7 is shown that, when ANC was activated, the SPL reduction at planes B and C ranges from 9 db to 24 db for distance up to 20cm far from the headrest. At plane B the length of the quiet zone is even bigger and reaches 30cm. At planes A and D, the noise attenuation gets worse similar to the first experiment. However, especially for the plane A the SPL reduction is about 10 db around the passenger's ears, which is sufficient to ensure the enhancement of passenger's experience. The significant attenuation of the two frequencies that form the beat signal around the ears is depicted in figure 8. The attenuation of the frequency at 110 Hz is around 12 db and the attenuation of 114 Hz varies from 7db to 17 db at the right ear of the passenger.

4 Conclusions

This manuscript introduces a simple multichannel ANC scheme for the attenuation of narrowband noise produced by the propellers of a small aircraft. The system consists of three parallel adaptive notch filters and is able to control three frequencies. Moreover, a linear extrapolation technique is used in order to relocate the quiet zone far from the error microphones and ESPRIT method has been chosen as a frequency estimator for the reference signal. The ANC system was experimentally tested for one tone signal and a beat signal as primary sound disturbance. The results show a significant attenuation of narrowband noise in a large area and the creation of a quiet zone that allows big freedom of movement for the passenger's head. In addition, ESPRIT algorithm estimates in a satisfactory way the frequencies of the reference signal and doesn't create any problems in the convergence of the ANC algorithm.

Acknowledgements

This research has been co-financed by the European Union and Greek national funds through the Horizon 2020 / Clean Sky JU, under the call H2020-CS2-CFP10-2019-01 (Clean Sky), Topic JTI-CS2-2019-CFP10-AIR-02-82, type of action CS2-RIA, project PIANO: Path Identification for Active Noise Control (project number 885976).

References

- [1] Johansson, S.; Nordebo, S.; Sjosten, P.; Lago T. L.; Claesson, I. Performance of a multiple versus a single-reference MIMO ANC algorithm based on a Dornier 328 test data set. *Proceedings of ATIVE 97, the 1997 international symposium of active control of sound and vibration*, Budapest, 1997.
- [2] Haase, T.; Unruh O.; Algermissen, S.; Pohl, M. Active control of counter-rotating open rotor interior noise in a Dornier 728 experimental aircraft. *Journal of Sound and Vibration*, Vol 376, 2016, pp 18-32.
- [3] Ross C. F. Active noise control in aircraft cabins. *The Journal of Acoustical Society of America*, Vol 105, 1999.
- [4] Siswanto, A.; Chang, C.; Kuo, S.M. Active noise control for headrests. *Proceedings of APSIPA annual summit and conference*, Hong Kong, 2015, pp 688-692.
- [5] Pabst, O.; Kletschkowski, T.; Delf, S. Active noise control in light jet aircraft. *The Journal of the Acoustical Society of America*, Vol 123, 2008.
- [6] Wang, H.; Sun, H.; Sun, Y.; Wu, M.; Yang, J. A narrowband active noise control system with frequency estimation algorithm based on parallel notch filter. *Signal Processing*, Vol 154, 2019, pp 108-119.
- [7] Yang, F.; Gupta, A.; Kuo, S.M. Parallel multifrequency active noise control systems. *Proceedings of the IEEE International Conference on Acoustics, Speech, and Signal Processing, ICASSP 2009*, Taipei, 2009.

- [8] Kuo, S.M.; Morgan, D.R. *Active noise control systems: Algorithms and DSP implementations*, Wiley, New York, 1996.
- [9] Jeon, H.J.; Chang, T.G.; Yu, S.; Kuo, S.M. A narrowband active noise control system with frequency corrector. *IEEE transactions on audio, speech and language processing*, Vol 19 (4), 2011.
- [10] Xiao, Y. A new efficient active noise control system and its performance analysis. *IEEE transactions on audio, speech and language processing*, Vol 17 (7), 2011.
- [11] Moreau, D.; Cazzolato, B.; Zander, A.; Petersen C. *A review of virtual sensing algorithms for active noise control*, Algorithms, Vol 1 (2), 2008, pp 69-99.
- [12] Paulraj, A.; Roy, R.; Kailath, T. Estimation of signal parameters via Rotational invariance techniques-ESPRIT. *Nineteenth Asilomar conference on circuits, systems, and computers*, Pacific Grove, 1985.
- [13] Besson, O.; Stoica, P.; Analysis of MUSIC and ESPRIT frequency estimates for sinusoidal signals with lowpass envelopes. *IEEE Transactions on Signal Processing*, Vol 44 (9), 1996.
- [14] Proakis, J.; Manolakis, D.; *Digital signal processing, principles, algorithms and application*, Prentice Hall, 4th edition, 2007.